Photodissociation Dynamics of Formic Acid at 206 nm

Tae Yeon Kang and Hong Lae Kim*

Department of Chemistry, College of Natural Sciences, Kangwon National University, Chuncheon 200-701, Korea
**E-mail: hlkim@kangwon.ac.kr*
Received July 24, 2006

The photodissociation dynamics of formic acid (HCOOH) at 206 nm have been investigated from rotationally resolved laser induced fluorescence spectra of OH ($^2\Pi$) fragments produced exclusively in the ground state. From the spectra, the rotational energy of the fragments was measured to be 820 ± 50 cm^{-1}. The translational energy released in the products, which is 87% of the total available energy of the system, was also measured from analyses of the Doppler profiles. Joining these data with quantum chemical molecular orbital calculations, we have concluded that the dissociation should take place along the S_1 surface with an exit channel barrier and also that the energy partitioning is determined at the exit channel.

Key Words : Formic acid, Photodissociation dynamics, Laser induced fluorescence

Introduction

The chemistry of formic acid (HCOOH) is of fundamental interest because it is an important intermediate in the oxidation of unsaturated hydrocarbons in combustion and the most abundant organic pollutant in Earth's atmosphere. In understanding atmospheric chemistry, the structures and dynamics of molecules in the excited electronic states are of special importance. Among organic molecules in our atmosphere, HCOOH has drawn the most attention because it is the simplest carboxylic acid whose spectroscopy and dynamics can be studied experimentally and theoretically in detail, casting it as a model for the study of larger carboxylic acids. In UV spectroscopy, the absorption spectrum of HCOOH shows some vibrational structures superimposed by continuous absorption starting from about 250 nm, which is assigned as the $n \rightarrow \pi^*_{C=O}$ electronic transition typical for simple carbonyl compounds.[1-3] The photophysical and photochemical processes from this ($n\pi^*$) state should depend upon the nature of the excited state and the shape of potential energy surfaces. The potential energy surfaces can be constructed in detail by quantum chemical calculations, but for the excited electronic states, such construction is extremely difficult due to multichannel interferences. However, the electronic absorption spectra and photodissociation dynamics can provide some information on the shape of potential energy surfaces in the excited electronic states.

The photodissociation of formic acid in the first UV absorption band has been extensively studied.[4-10] The major primary dissociation channel has been found to produce the CHO and OH radicals with a quantum yield of 0.7-0.8 at 222 nm.[11] However, at longer wavelengths, the lifetime of the molecule in the excited state is a few tens of nanoseconds, manifested by the rotationally resolved spectra of the 0^0_0 and 3^1_0 bands measured by the laser induced fluorescence technique.[12,13] In fact, at 248 nm, H_2O, CO, and CO_2 products were found by time-resolved Fourier Transform Infrared spectroscopy; they are also the products in the thermal decomposition of HCOOH.[14,15] At this wavelength, the photon energy is not high enough to overcome the barrier for dissociation in the S_1 excited state; thus, the dissociation takes place mainly in the vibrationally hot ground electronic state after internal conversion. As the photon energy increases, the lifetime becomes shorter and several dissociation channels in the excited electronic states, such as CHO + OH and H atom dissociation channels, are open. At shorter wavelengths, most of the available energy (about 80%) was found to be distributed in the product translation and internally cold products were observed. Previous reports suggest that the dissociation should be predissociative and the potential energy surface leading to the CHO and OH radical products has an exit channel barrier. Similar to HCOOH, the photodissociation of acetaldehyde in UV takes place along the triplet surface with an exit channel barrier.[16-18] When the photon energy is close to the dissociation barrier, internally cold CHO and CH_3 radical products are observed, whereas the rotational energy of the CHO products increases as the photon energy increases. To understand the detailed dynamics of the photodissociation of HCOOH in relation to the potential energy surfaces, more of the dissociation dynamics should be investigated at other wavelengths along the UV absorption band together with theoretical calculations on the nature of the electronic transition, potential energy surfaces and other key characteristics.

In the present study, the photodissociation dynamics of formic acid at 206 nm have been investigated by measuring rotationally resolved laser induced fluorescence spectra of OH fragments produced exclusively in the ground electronic state. From these spectra, the energy partitioning in the products was determined. Along with the results of the quantum chemical molecular orbital calculations, the detailed dynamics of the dissociation processes are discussed.

Experiments

The experiments were carried out in a low pressure flow

cell with conventional photolysis-probe geometry.[8] The cell, a cube made of stainless steel with four arms (each 30 cm long), was evacuated to a pressure of 10^{-5} Torr by a mechanical pump. The gaseous sample in equilibrium with liquid HCOOH at ambient temperature was slowly flowed through the cell at a pressure of 60 mTorr. The pressure was controlled by two needle valves. The liquid HCOOH (stated purity of 98%) was purchased from Aldrich and used without further purification.

The 206 nm, horizontally polarized photolysis light (2 mJ/pulse, 4 mm dia.) was generated by frequency doubling (with a BBO crystal) of a dye laser (ND-6000, Continuum) output at 412 nm generated by pumping with 355 nm light, the third harmonic of an Nd:YAG laser (Surelite, Continuum). The probe light to measure the laser-induced fluorescence spectra of OH, employing the $X(^2\Pi) \rightarrow A(^2\Sigma)$ electronic transition at 306-320 nm, was a doubled output of another dye laser (HD-500, Lumonics) pumped by the second harmonic of an Nd:YAG laser (YM-800, Lumonics). The two laser beams were collinearly or perpendicularly introduced to the cell through the arms, which contain baffles to minimize scattered radiation. The delay between the photolysis and probe, typically about 100 ns, was controlled with a digital pulse and delay generator. The power of the probe light, which was about 30 μJ/pulse (~4 mm dia.), was kept as low as possible to avoid saturation in the spectra.

The fluorescence signal was detected with a photomultiplier tube (R-212UH, Hamammatsu) perpendicularly mounted relative to the two laser beams through cut-off filters and a collection lens. The measured signal was fed to boxcars and processed with a signal processor. A 60 mTorr sample pressure and 100 ns time delay between the photolysis and probe ensures nascent product energy distribution. The fluorescence spectra were corrected with variation of the photolysis and probe laser powers, and the data were collected and stored on a personal computer.

The linewidth of the laser output was measured by rotationally resolved gaseous I_2 spectra near 620 nm, which was found to be 0.07 cm^{-1} at FWHM. This laser line profile was deconvoluted from the measured line profiles to estimate the actual Doppler profiles in the spectra.

Results and Discussion

A portion of the laser induced fluorescence spectra of $OH(^2\Pi)$ produced from photodissociation of HCOOH is presented in Figure 1. In the liquid sample of formic acid, an appreciable amount of hydrogen-bonded dimers of formic acid should be present, but quantum yield measurements of OH production from photodissociation of gaseous formic acid showed no OH yield from the dimers.[19] The spectrum shows well-resolved P-, Q-, and R- branch rotational lines of the 0-0 band, which were assigned according to Dieke and Crosswhite.[20] However, no appreciable fluorescence intensities were detected out of the noise in the 1-1 band region of the spectrum, which suggests negligible vibrational excitation of the OH fragments. In Figure 2, normalized rotational

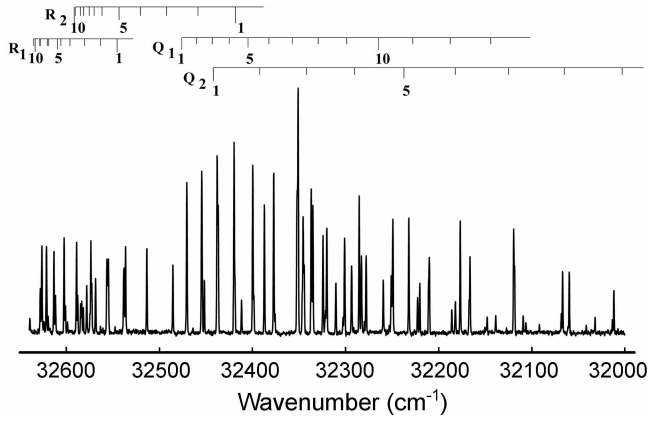

Figure 1. Portion of Laser induced fluorescence spectrum of OH produced from photodissociation of formic acid at 206 nm employing the A-X transition.

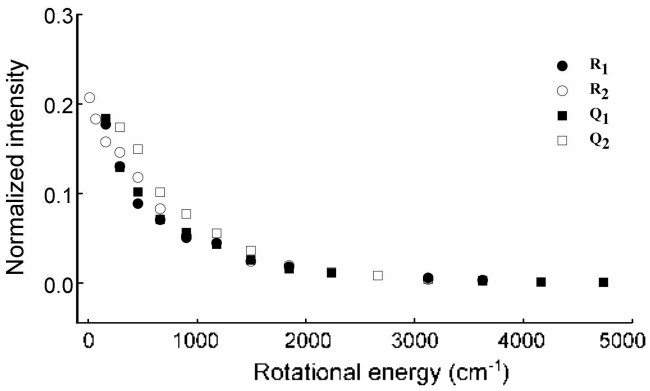

Figure 2. Normalized rotational population distribution obtained from the spectrum in Figure 1 as a function of rotational energy.

population distributions obtained by relative intensities of the individual lines corrected by appropriate line strength factors are presented.[21] From this data the average rotational energy of OH was found to be 820 ± 50 cm^{-1}. The Doppler

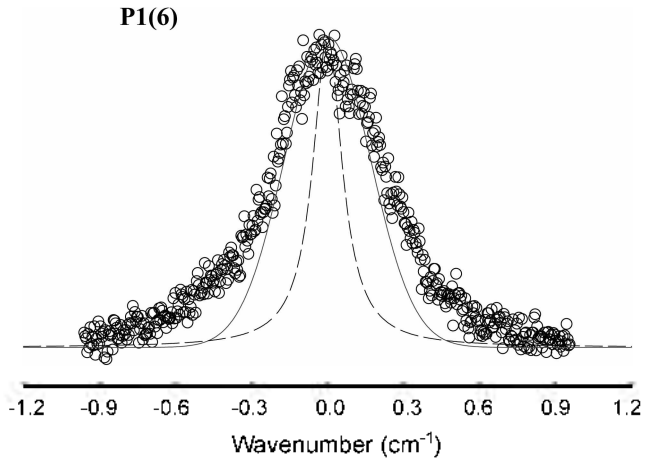

Figure 3. Doppler profile of the $P_1(6)$ rotational transition in the spectrum in Figure 1. Circles are from the experiment, dashed line is the laser line profile, and solid line is the actual Doppler profile obtained from deconvolution of the laser line profile from the measured.

broadened $P_1(6)$ rotational line in the OH spectrum is presented in Figure 3. When the two laser beams are collinearly propagated, the polarization direction of the photolysis light is perpendicular to the probe direction; whereas when the two laser beams are introduced perpendicular to each other, the polarization direction of the photolysis light becomes parallel to the probe direction. However, from these two different experimental pump-probe geometries, the same Doppler profiles were observed, which were Gaussian-like profiles implying the isotropic angular distribution of the fragments. From the observed one-dimensional Doppler broadened spectra, the average translational energies of the OH fragments were measured from the second moment of the profile after deconvolution of the laser line profile.[22] The average center of mass translational energy release in the products for the OH rotational state N=6 was then calculated to be $9,000 \pm 500$ cm^{-1}, invoking energy and momentum conservation. The fraction of the translational energy in the total available energy is 0.87, as listed in Table 1 with values from other experiments.

To understand the details of the dissociation mechanism, spin correlation arguments would be helpful. Since the OH products are in the $^2\Pi$ state, which is two-fold degenerate, and the CHO products are in the $^2A'$ state, the four dissociating molecular states should be the two singlet states, S_0 and S_1, and the two triplet states, T_1 and T_2. Thus, the dissociation would occur from either the ground singlet state after internal conversion from the S_1 state, from the excited singlet state, or from the triplet states after relaxation from the initially excited singlet state. When the dissociation takes place in the ground singlet state after the internal conversion, a statistical energy partitioning resulting from excessive vibrational energy redistribution would be expected because the molecules are in the highly vibrationally excited states, like thermal decomposition. In addition, the major decomposition products from the ground singlet state are known to be molecular products, such as H_2O, CO_2, and CO. The unusually large translational energy released in our study resulted in a non-statistical energy partitioning in the products, which implies that dissociation should occur in the excited electronic states.

In Figure 4, the Λ-doublet distribution of the OH fragments, showing close to statistical distribution is presented. In diatomic molecules in the Π state as OH in $^2\Pi$, an unpaired p_π orbital lies perpendicular to the molecular axis. Since the electronic angular momentum has $\Lambda = \pm 1$ projections with respect to the molecular axis in this case, the rotational states are split into two because of interactions between the electronic and rotational angular momentum when the molecules rotate. In the classical limit, the wavefunction of the unpaired electron in the p_π orbital can be approximated as a lobe. When this lobe lies in the plane of molecular rotation, the wavefunction is symmetric with respect to the plane, which forms the Π(A') or Π^+ state among the two Λ-doublet states, whereas the wavefunction is antisymmetric, the Π(A") or Π^- state, when the lobe lies perpendicular to the plane. The propensity of the dissociation products in one of the two Λ-doublet states originates from conservation of the direction of the unpaired p_π orbital lobe generated by nuclear motion, that is, bond cleavage along the reaction coordinate. When the parent molecule does not rotate or the dissociation takes place faster than the rotational period of the parent molecule, such as in the case of direct dissociation from a repulsive state, the dissociation takes place in the plane, resulting in the products exclusively in the Π^- state. This propensity decreases as the dissociation time becomes longer, resulting in rotation of the parent molecule, which also happens if there are any dynamical constraints, such as excessive torsional vibrational motion of the parent molecule. The fact that negligible propensity in the Λ-doublet distribution of OH was observed in this experiment suggests that the dissociation time is relatively long and some barrier in the course of dissociation along the S_1 or the triplet surfaces.

Table 1. Energy partitioning in products from photodissociation of formic acid at various wavelengths

	193 nm[a]	225 nm[b]	206 nm
E_{av} (cm^{-1})	14,110	6,820	10,300[c]
$<f_t(OH)>$	0.05	0.065	0.080
$<f_t(sys)>$	0.82	0.84	0.87

[a]ref. 8. [b]ref. 6. [c]$E_{av} = h\nu(206\ nm) + 3/2\ RT - D_0$

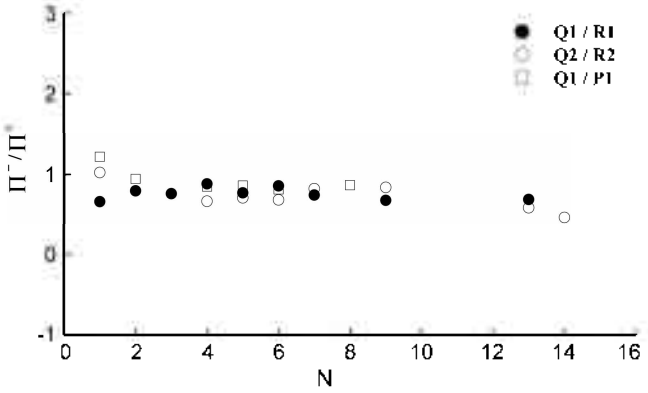

Figure 4. Λ-doublet distribution of OH produced from photodissociation of formic acid at 206 nm as a function of rotational quantum number N.

To figure out the shape of the potential energy surfaces in the excited electronic state, quantum chemical molecular orbital calculations were considered, especially for the S_1 and T_1 states along the reaction coordinate. According to the complete active space self-consistent field/multireference configuration interaction (CASSCF/MR-CI) calculations by Fang and coworkers,[10] the S_1 and T_1 surfaces along the reaction coordinates have barriers of 56.5 and 62.8 kJ/mol relative to the S_1 and T_1 origin, respectively (Figure 5). In addition, they found the crossing point between the S_1 and the T_1 surfaces, from which the transition probability of intersystem crossing between S_1 and T_1 was estimated to be 5.5×10^{-4}, employing the Landau-Zener model. The negligible interaction between the S_1 and T_1 states results in the non-

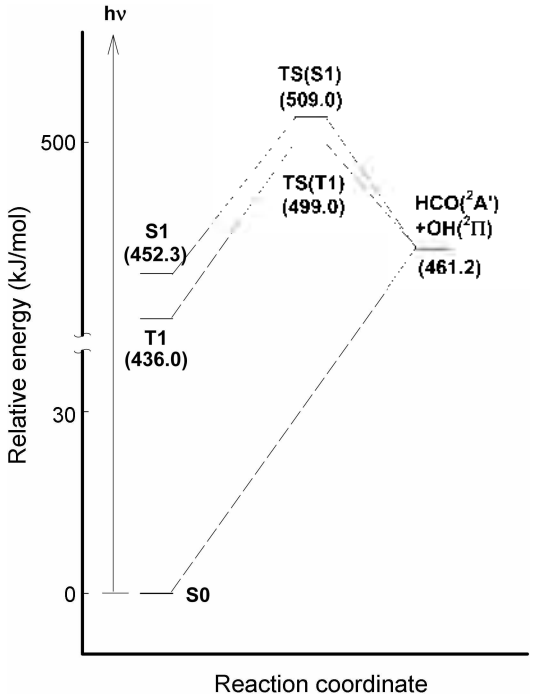

Figure 5. Schematic energy level diagram of photodissociation of formic acid producing OH and HCO adapted from reference 10 and thermochemical data from reference 24.

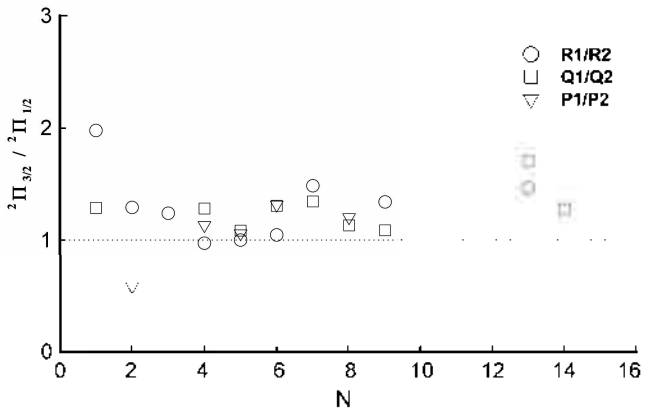

Figure 6. Spin-orbit fine structure distribution of OH in the $^2\Pi$ state produced from photodissociation of formic acid at 206 nm as a function of rotational quantum number N.

statistical population distribution of the two spin-orbit states in OH, as observed in the experiment (Figure 6). This non-statistical spin-orbit population distribution of OH is also observed in the 212.8 nm photodissociation of formic acid.[9] The higher barrier along the T_1 surface and the negligible interaction between S_1 and T_1 suggest that the dissociation should take place on the excited singlet surface not the triplet surfaces.

The first electronic absorption band of HCOOH in UV, starting from around 250 nm shows sharp structures at a long wavelength region superimposed by continuous absorption, with a peak around 215 nm. The transition is assigned as the n(3a") $\rightarrow \pi^*$(10a') transition primarily localized in the C=O moiety. The structured transitions in this band are long progressions of the C=O stretching (ν_3) and the O-C-O bending (ν_2) vibrations, resulting from structural changes from the planar to the pyramidal structure upon absorption, a result of the molecular orbital interactions mentioned by Walsh.[23] Since the transition is vibronically allowed through ν_3 and ν_2, the direction of the transition dipole moment has all three components in space, resulting in isotropic angular distribution of the fragments. Upon excitation of the sharp peaks on the long wavelength side of the absorption band, it has been found that most of the available energy is transformed into product translation and the energy partitioning is insensitive to the initial state selection.[15] At 206 nm, the short wavelength side of the absorption band, the available energy is the photon energy, 585.0 kJ/mol (including the internal energy of the parent molecule) minus the dissociation energy, 461.2 kJ/mol,[24] which is 123.8 kJ/mol. The fraction of the available energy going into product translation is 0.87, whereas the fraction of the rotational energy in OH is 0.080. The low vibrational excitation of OH is consistent with the localized transition in the C=O moiety, with almost no change in the O-H bond length at the Franck-Condon region at the transition state. When we assume that the energy partitioning would be determined at the transition state, most of the available energy would be transformed into product translation and the rotational energy of the fragments can be predicted employing an impulsive model.[25] The fraction of rotational energy in OH according to the impulsive model is calculated to be 0.03. The origin of the rotational energy of OH is an impulsive force upon dissociation, resulting in planar dissociation and torsional vibrational motion of the parent molecule, which results in a plane of rotation perpendicular to the dissociation axis. The observed statistical Λ-doublet distribution should also reflect these two contributions. Upon excitation at 206 nm, the measured energy partitioning is similar to those from excitation at longer wavelengths. At this wavelength, the initial excitation still induces many quanta in the C=O vibration in the Franck-Condon region of the potential energy surface from which the dissociation proceeds along the C=O vibrationally adiabatic curves strongly coupled to the reaction coordinate, where the barrier is present in the exit channel. In this case, the energy partitioning among products should be determined at the transition state and most of the available energy is expected to be transformed into product translation as observed in this experiment.

Acknowledgments. This work was funded by the Korea Research Foundation (C00221).

References

1. Ng, T. L.; Bell, S. *J. Mol. Spectros.* **1974**, *50*, 166.
2. Demoulin, D. *Chem. Phys.* **1976**, *17*, 471.
3. Fridh, C. *J. Chem. Soc. Faraday Trans. II* **1978**, *74*, 190.
4. Ebata, T.; Fujii, A.; Amano, T.; Ito, M. *J. Phys. Chem.* **1987**, *91*, 6095.
5. Brouard, M.; O'Mahony, J. *Chem. Phys. Lett.* **1988**, *149*, 45.
6. Ebata, T.; Amano, T.; Ito, M. *J. Chem. Phys.* **1989**, *90*, 112.

7. Langford, S. R.; Batten, A. D.; Kono, M.; Ashfold, M. N. R. *J. Chem. Soc. Faraday Trans.* **1997**, *93*, 3757.
8. Shin, S. K.; Han, E. J.; Kim, H. L. *J. Photochem. Photobiol. A Chemistry* **1998**, *118*, 71.
9. Lee, K. W.; Lee, K. S.; Jung, K. H.; Volpp, H. R. *J. Chem. Phys.* **2002**, *117*, 9266.
10. He, H. Y.; Fang, W. H. *J. Am. Chem. Soc.* **2003**, *125*, 16139.
11. Singleton, D. L.; Paraskevopoulos, G.; Irwin, R. S. *J. Phys. Chem.* **1990**, *94*, 695.
12. Ioannoni, F.; Moule, D. C.; Clouthier, D. J. *J. Phys. Chem.* **1990**, *94*, 2290.
13. Brouard, M.; Simons, J. P.; Wang, J. X. *Faraday Discuss. Chem. Soc.* **1991**, *91*, 63.
14. Su, H.; He, Y.; Kong, F.; Fang, W.; Liu, R. *J. Chem. Phys.* **2000**, *113*, 1891.
15. Borges, Jr. I.; Rocha, A. B.; Martinez-Nunez, E.; Vazquez, S. *Chem. Phys. Lett.* **2005**, *407*, 166.
16. Leu, G. H.; Huang, C. L.; Lee, S. H.; Lee, Y. C.; Chen, I. C. *J. Chem. Phys.* **1998**, *109*, 9340.
17. Cruse, H. A.; Softley, T. P. *J. Chem. Phys.* **2005**, *122*, 124303.
18. Thompson, K. C.; Crittenden, D. L.; Kable, S. H.; Jordan, M. J. T. *J. Chem. Phys.* **2006**, *124*, 44302.
19. Jolly, G. S.; Singleton, D. L.; Paraskevopoulos, G. *J. Phys. Chem.* **1987**, *91*, 3463.
20. Dieke, G. H.; Crosswhite, H. M. *J. Quant. Spectros. Radiat. Transfer* **1962**, *2*, 97.
21. Chidsey, I. L.; Crosley, D. R. *J. Quant. Spectros. Radiat. Transfer* **1980**, *23*, 187.
22. Kang, T. Y.; Shin, S. K.; Kim, H. L. *Bull. Korean Chem. Soc.* **2004**, *25*, 1130.
23. Walsh, A. D. *J. Chem. Soc. (London)* **1953**, *1953*, 2306.
24. Atkinson, R.; Baulch, R. A.; Hampson Jr., R. F.; Kerr, J. A.; Rossi, M. J.; Troe, J. *J. Phys. Chem. Ref. Data* **1999**, *28*, 191.
25. Busch, G. E.; Wilson, K. R. *J. Chem. Phys.* **1972**, *56*, 3626.